

# Low Temperature Precursor Route for Highly Efficient Spherically Shaped LED-Phosphors $M_2Si_5N_8:Eu^{2+}$ ( $M = Eu, Sr, Ba$ )

Martin Zeuner, Frauke Hintze, and Wolfgang Schnick\*

Department Chemie und Biochemie, Ludwig-Maximilians-Universität München, Butenandtstrasse 5-13 (D), D-81377 München, Germany

Received September 12, 2008. Revised Manuscript Received November 19, 2008

The highly efficient nitridosilicate phosphors  $M_2Si_5N_8$  ( $M = Sr, Ba, Eu$ ) for phosphor-converted pc-LEDs were synthesized at low temperatures using a novel precursor route involving metal amides  $M(NH_2)_2$ . These precursors have been synthesized by dissolution of the respective metals in supercritical ammonia at 150 °C and 300 bar. The thermal behavior and decomposition process of the amides were investigated with temperature programmed powder X-ray diffractometry and thermoanalytical measurements (DTA/TG). These investigations rendered the amides as suitable intermediates for reaction with silicon diimide ( $Si(NH)_2$ ). Thus, the desired nitridosilicate phosphors were obtained at relatively low temperatures around 1150–1400 °C which is approximately 300 °C lower compared to common synthetic approaches starting from metals or oxides. The influence of the thermal treatment on the phosphor morphology has been studied extensively. The accessibility of spherical phosphor particles represents another striking feature of this route since it improves light extraction from the crystallites due to decreasing light guiding and decreasing re-absorption inside the phosphor particle. The synthesized luminescent materials  $M_2Si_5N_8:Eu^{2+}$  ( $M = Sr, Ba$ ) exhibit quantum efficiencies and emission band widths (FWHM 70–90 nm) comparable to standard phosphor powders. Employment of  $Eu(NH_2)_2$  as dopant reagent for synthesis of  $Ba_2Si_5N_8:Eu^{2+}$  proved favorable for the formation of spherical crystallites compared to doping with Eu metal, halides, or oxide.

## Introduction

In the last years there has been great interest in nitridosilicates, oxonitridosilicates (sions), and oxonitridoaluminosilicates (sialons) due to their remarkable thermal, mechanical, and chemical stability as well as their structural diversity.<sup>1,2</sup> Nitridosilicates extend the structural variety of the naturally occurring oxosilicates because nitrogen atoms can connect two, three, or even four silicon atoms to form highly condensed network structures.<sup>3</sup> Furthermore, edge-sharing of neighboring tetrahedra to form  $Si_2N_6$  units occurs in nitridosilicates as well.<sup>4,5</sup> Recently, nitridosilicates and oxonitridosilicates have emerged as promising host lattices for rare-earth-doped luminescent materials in phosphor-converted LEDs (pc-LEDs).<sup>6–10</sup> Particularly,  $Eu^{2+}$ -doped nitridosilicates  $M_2Si_5N_8$  with  $M = Ca, Sr, or Ba$ <sup>11,12</sup> (the so-called 2-5-8 materials) are now being industrially used in

pc-LEDs as highly efficient red phosphor materials.<sup>8,13</sup> They afford conversion of the initial blue radiation of GaN-based primary LEDs into red light, thus, in combination with a green to yellow emitting converter material, achieving warm white light pc-LEDs with improved color rendition in the red spectral region.<sup>6</sup> The low energy excitation and emission bands of these compounds are mainly due to the strong nephelauxetic effect of the covalently bound nitrogen coordinating the alkaline earth ions and  $Eu^{2+}$ .<sup>13</sup> The 2-5-8 phases with Sr, Ba,<sup>14</sup> and Eu<sup>15</sup> crystallize isotypically in the space group  $Pmn2_1$ . The crystal structure is based on a network of corner sharing  $SiN_4$  tetrahedra where half of the nitrogen atoms connect two ( $N^{[2]}$ ) and the other ones three Si atoms ( $N^{[3]}$ ).

Hence, much effort has been directed towards the synthesis of new nitridosilicates as host systems and more efficient synthetic approaches of these important materials. Commonly, nitridosilicates have been synthesized using high-temperature reactions in the range of 1550–1650 °C starting

\* To whom correspondence should be addressed. Fax: (+49)89-2180-77440. E-mail: wolfgang.schnick@uni-muenchen.de.

- (1) Schnick, W. *Int. J. Inorg. Mater.* **2001**, *3*, 1267.
- (2) Schnick, W.; Huppertz, H. *Chem. Eur. J.* **1997**, *3*, 679.
- (3) Huppertz, H.; Schnick, W. *Z. Anorg. Allg. Chem.* **1997**, *623*, 212.
- (4) Huppertz, H.; Schnick, W. *Chem. Eur. J.* **1997**, *3*, 249.
- (5) Yamane, H.; DiSalvo, F. J. *J. Alloys Compd.* **1996**, *240*, 33.
- (6) Mueller-Mach, R.; Mueller, G.; Krames, M. R.; Höpfe, H. A.; Stadler, F.; Schnick, W.; Juestel, T.; Schmidt, P. *Phys. Status Solidi A* **2005**, *202*, 1727.
- (7) Xie, R.-J.; Hirosaki, N. *Sci. Technol. Adv. Mater.* **2007**, *8*, 588.
- (8) Xie, R.-J.; Hirosaki, N.; Kimura, N.; Sakuma, K.; Mitomo, M. *Appl. Phys. Lett.* **2007**, *90*, 191101/1.
- (9) Piao, X.; Horikawa, T.; Hanzawa, H.; Machida, K. *Appl. Phys. Lett.* **2006**, *88*, 161908.
- (10) Li, Y. Q.; deWith, G.; Hintzen, H. T. *J. Solid State Chem.* **2008**, *181*, 515.

- (11) Yamada, M.; Naitou, T.; Izuno, K.; Tamaki, H.; Murazaki, Y.; Kameshima, M.; Mukai, T. *Jpn. J. Appl. Phys.* **2003**, *42*, L20.
- (12) Höpfe, H. A.; Lutz, H.; Morys, P.; Schnick, W.; Seilmeier, A. *J. Phys. Chem. Solids* **2000**, *61*, 2001.
- (13) Schmidt, P.; Tuecks, A.; Meyer, J.; Bechtel, H.; Wiechert, D.; Mueller-Mach, R.; Mueller, G.; Schnick, W. *Proc. SPIE-Int. Soc. Opt. Eng.* **2007**, *6669*, 66690P/1–66690P/9 (Seventh International Conference on Solid State Lighting, 2007).
- (14) Schlieper, T.; Milius, W.; Schnick, W. *Z. Anorg. Allg. Chem.* **1995**, *621*, 1380.
- (15) Huppertz, H.; Schnick, W. *Acta Crystallogr., Sect. C* **1997**, *53*, 1751.

from metals or oxides and silicon nitride or silicon diimide.<sup>16</sup> Initially, the 2-5-8 phases have been obtained using a radio-frequency furnace convenient for high-temperature reactions.<sup>6,12,16</sup> However, the synthesis of  $\text{Sr}_2\text{Si}_5\text{N}_8$  has also been reported at temperatures around 1400–1500 °C using the method of carbothermal reduction and nitridation (CRN) of oxides.<sup>9</sup> A major disadvantage of the latter route is the inevitable formation of residual carbon as a byproduct which might reduce absorption and emission of the phosphor. Flux techniques (metallic sodium) at quite low temperatures (around 900–1100 °C) have been utilized for the synthesis of other nitridosilicates (e.g.,  $\text{MSiN}_2$ ); however, limitations occur due to the boiling temperature of the flux or the usage of closed reaction systems (e.g., tantalum ampoules)<sup>17</sup> hampering large-scale processing. Recently, the synthesis of the promising nitridoalumosilicate phosphor  $\text{CaAlSiN}_3\text{:Eu}^{2+}$  has been reported at low temperatures in supercritical ammonia starting from a pre-synthesized  $\text{CaAlSi}$  alloy. However, the latter approach requires a mineralizer to reach sufficient crystallinity.<sup>18</sup>

In this work, we present a novel approach to the nitrido-silicates  $\text{M}_2\text{Si}_5\text{N}_8$  ( $\text{M} = \text{Sr}, \text{Ba}, \text{Eu}$ ) at low temperatures around 1150 °C by usage of microcrystalline metal amide precursors  $\text{M}(\text{NH}_2)_2$  ( $\text{M} = \text{Sr}, \text{Ba}, \text{Eu}$ ) and reaction with silicon diimide ( $\text{Si}(\text{NH})_2$ ). The synthesis can be performed without further additives like flux or mineralizer and therefore reduces significantly contamination with other elements. This route allows reduction of the synthesis temperature of these phosphors by more than  $\sim 300$  °C compared to the common synthesis temperatures around  $\sim 1450$ – $1650$  °C. Furthermore, the influence of these precursors on the morphology and luminescent properties of the phosphors was investigated and compared with powders synthesized by conventional techniques. Additionally, the effect of using  $\text{Eu}(\text{NH}_2)_2$  as a dopant compared to “common” doping reagents like europium metal,  $\text{Eu}_2\text{O}_3$ , or  $\text{EuF}_3$  on the crystal shape was investigated.

## Experimental Section

Unless otherwise stated, all manipulations were performed with rigorous exclusion of oxygen and moisture in flame-dried Schlenk-type glassware on a Schlenk line, interfaced to a vacuum line ( $10^{-3}$  mbar), or in an argon-filled glovebox. Argon (Messer-Griesheim, 5.0) was purified by passage over columns of silica gel (Merck), molecular sieve (Fluka, 4 Å), KOH (Merck,  $\geq 85\%$ ),  $\text{P}_4\text{O}_{10}$  (Roth,  $\geq 99\%$ , granulate), and titanium sponge at 700 °C (Johnson Matthey, 99.5%, grain size  $\leq 0.8$  cm). Ammonia (Messer-Griesheim, 3.8) was predried by passage over columns of KOH (Merck,  $\geq 85\%$ ) and Cr(II)-oxide catalyst<sup>19</sup> and then condensed and stored over Na and K (both Merck, pieces) before use.

The general procedure for reactions in supercritical  $\text{NH}_3$  is described in the following: The starting material (strontium and barium, Sigma-Aldrich, 99.99%, pieces; europium, Smart-Elements, 99.9%, pieces) was introduced into a Parr high-pressure vessel

(Type 4740) with a Parr gage block (Type 4316) and connected to a vacuum/inert gas line. A sufficient amount of ammonia was condensed by cooling the vessel to  $-80$  °C. The reaction vessel was closed and slowly warmed up to room temperature and then heated at 10 °C/min to the final reaction temperature. A pressure of 300 bar was observed during the reaction. After 5 d the vessel was cooled down to room temperature and the pressure was reduced carefully by opening the valve of the unit. Finally, the vessel was opened in an argon-filled glovebox. A finely crystalline product was isolated and analyzed by IR spectroscopy and powder XRD (Stoe STADI P diffractometer; transmission mode,  $\text{Mo K}\alpha_1$  radiation,  $\lambda = 0.7104$  Å).

Synthesis of  $\text{M}_2\text{Si}_5\text{N}_8\text{:Eu}$  ( $\text{M} = \text{Sr}, \text{Ba}, \text{Eu}$ ) is described as follows: A mixture of stoichiometric amounts of  $\text{M}(\text{NH}_2)_2$  with  $\text{M} = \text{Sr}, \text{Ba}, \text{Eu}$  and silicon diimide (synthesized according to the literature)<sup>20</sup> was placed in a tungsten crucible under an argon atmosphere inside a glovebox (Unilab, MBraun, Garching,  $\text{O}_2 < 0.1$  ppm,  $\text{H}_2\text{O} < 0.1$  ppm). After placing the crucible into the water-cooled quartz reactor of a radio-frequency furnace (type IG 10/200 Hy, frequency: 200 kHz, max. electrical output: 12 kW, Hüttinger, Freiburg)<sup>16</sup> under a  $\text{N}_2$  atmosphere, the temperature was raised to 800 °C within 60 min. After 3 h the temperature was increased to 1150–1400 °C within 1 h and maintained for 24 h. Slow cooling to 800 °C within 12 h and quenching to room temperature in 30 min yielded  $\text{M}_2\text{Si}_5\text{N}_8$  ( $\text{M} = \text{Sr}, \text{Ba}, \text{Eu}$ ). The identity and phase purity of the product was verified by X-ray powder diffraction. The samples  $\text{Eu}_2\text{Si}_5\text{N}_8$  and  $\text{Sr}_2\text{Si}_5\text{N}_8$  have been proven to be single phase, and the X-ray diffraction patterns of undoped and doped  $\text{Eu}_2\text{Si}_5\text{N}_8$ ,  $\text{Sr}_2\text{Si}_5\text{N}_8$  and  $\text{Ba}_2\text{Si}_5\text{N}_8$  powders are in good agreement with the reported powder patterns in JCPDS 87-423, 85-101, and 85-102, respectively (see Supporting Information). The X-ray powder patterns have also been double-checked by comparison with theoretical diffraction patterns calculated from single crystal X-ray diffraction data.<sup>14,15</sup>

High-temperature in situ X-ray diffractometry was performed on a STOE Stadi P powder diffractometer (Ge(111)-monochromated  $\text{Mo K}\alpha_1$  radiation,  $\lambda = 0.7104$  Å) with an integrated furnace, using sealed silica capillaries ( $\varnothing 0.3$  mm). The samples were heated from 20 to 1000 °C in steps of 50 °C using a heating rate of  $3$  °C $\cdot\text{min}^{-1}$ .

Scanning electron microscopy was performed on a JEOL JSM-6500F equipped with a field emission gun at an acceleration voltage of 10 kV. Samples were prepared by placing the powder specimen on adhesive conductive pads and subsequently coating them with a thin conductive carbon film. Each EDX spectrum (Oxford Instruments) was recorded with the analyzed area limited on one single nanocrystal to avoid the influence of possible contaminating phases.

FTIR measurements were carried out on a Bruker IFS 66v/S spectrometer. The preparation procedures were performed in a glovebox under dried argon atmosphere. Spectra were recorded at ambient conditions in the range between 400 and 4000  $\text{cm}^{-1}$  by dispersing the samples in anhydrous KBr pellets.

Excitation and emission spectra for powdered samples of the as-prepared reaction products of  $\text{M}_2\text{Si}_5\text{N}_8\text{:Eu}$  ( $\text{M} = \text{Sr}, \text{Ba}$ ) were measured at Philips research laboratories, Aachen, by means of an in-house built spectrometer system equipped with a 150-W Xe arc lamp, a  $2 \times 500$  mm Czerny Turner monochromator, 1800 grooves/mm, 250/500 nm blaze gratings, and a SPC multiplier detection unit (modified FL900, Edinburgh Instruments, U.K.).<sup>21</sup> For the calculation of CIE (Commission Internationale d'Eclairage) color coordinates ( $x, y$ ) the emission spectra were weighted by the  $10^6$

(16) Schnick, W.; Huppertz, H.; Lauterbach, R. *J. Mater. Chem.* **1999**, *9*, 289.

(17) Gál, Z. A.; Mallinson, P. M.; Orchard, H. J.; Clarke, S. J. *J. Inorg. Chem.* **2004**, *43*, 3998.

(18) Li, J.; Watanabe, T.; Sakamoto, N.; Wada, H.; Setoyama, T.; Yoshimura, M. *Chem. Mater.* **2008**, *20*, 2095.

(19) Krauss, H. L.; Stach, H. Z. *Anorg. Allg. Chem.* **1969**, *366*, 34.

(20) Lange, H.; Wötting, G.; Winter, G. *Angew. Chem.* **1991**, *103*, 1606; *Angew. Chem. Int. Ed. Engl.* **1991**, *30*, 1579.

(21) Jüstel, T.; Krupa, J.-C.; Wiechert, D. U. *J. Lumin.* **2001**, *93*, 179.

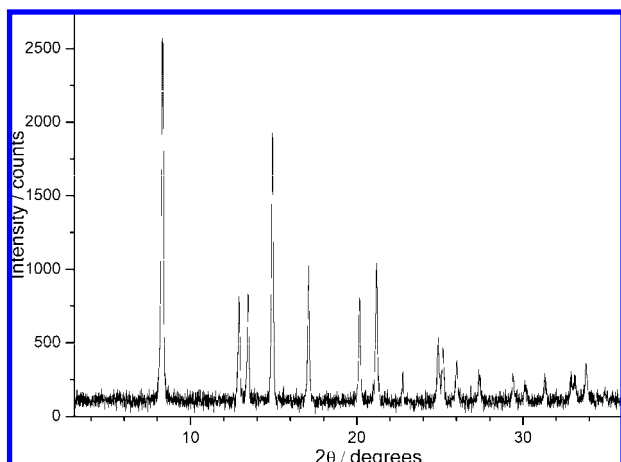


Figure 1. XRD pattern (Mo  $K\alpha_1$ ) of  $Sr(NH_2)_2$ , background subtracted.

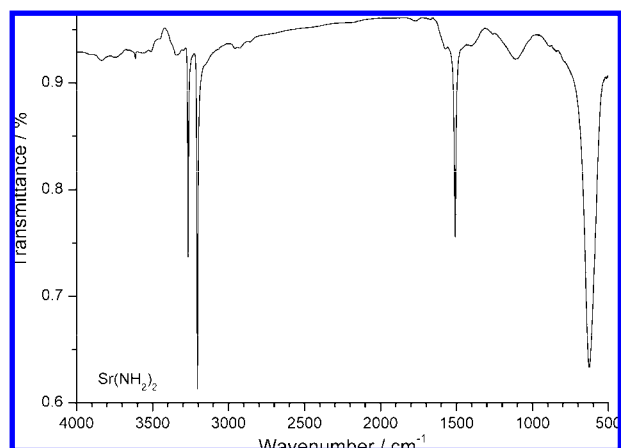


Figure 2. IR spectrum of  $Sr(NH_2)_2$ .

standard observer CIE color matching functions. After summarizing, the obtained tri-stimulus values were normalized to obtain CIE 1933 color coordinates.

TG/DTA measurements were performed on a TGA 92-2400 (Setaram) thermoanalyzer equipped with gage heads. The samples were placed in an unsealed  $Al_2O_3$  crucible and heated from RT to 700 °C with a heating rate of 5 °C · min<sup>-1</sup> (gas flow 100 mL · min<sup>-1</sup> helium 5.0).

## Results and Discussion

The precursor amides  $M(NH_2)_2$  ( $M = Eu, Ba, Sr$ ) can be synthesized by dissolving the corresponding metals in liquid ammonia according to Senker et al. (liquid route).<sup>22</sup> The use of supercritical ammonia (sc- $NH_3$ ) in a high-pressure autoclave (Parr; Type 4740) is performed at higher temperatures and pressures and thus allows faster reaction times compared to the conventional liquid  $NH_3$  route at normal pressure. Phase pure and colorless  $Sr(NH_2)_2$  was obtained in supercritical ammonia after 5 d at 150 °C and 300 bar. The XRD pattern and IR spectrum are depicted in Figures 1 and 2, respectively. The XRD pattern indicated the complete formation of  $Sr(NH_2)_2$  without any observable metal residues (JCPDS 16-477). The IR spectrum proves the presence of N–H groups in the amide, visible at the vibrational bands

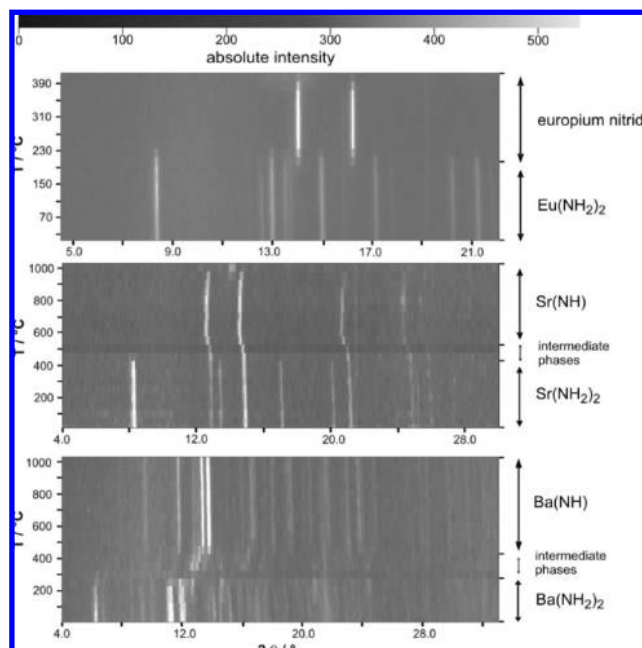


Figure 3. High-temperature in situ X-ray diffractometry (Mo  $K\alpha_1$ ) of  $M(NH_2)_2$  ( $M = Eu, Sr, Ba$ ).

at 3267, 3205 (N–H stretching) and 1509  $cm^{-1}$  (N–H deformation).<sup>23</sup> The sc- $NH_3$  approach was also applied to the synthesis of  $Ba(NH_2)_2$  and  $Eu(NH_2)_2$  with quite comparable analysis results which, however, are not presented in detail. Europium amide is obtained as a brown powder from the liquid route while the sc- $NH_3$  approach leads to orange  $Eu(NH_2)_2$ . This is due to the fact that a more complete reaction is observed in sc- $NH_3$  while the reaction in liquid ammonia leaves impurities like  $EuH_2$  which are detectable in the XRD pattern as well as some non-reacted metal. The sc- $NH_3$  approach is well suited for the synthesis of large amounts of a number of amides of electropositive metals.

The metal amides turned out to be very promising precursors because decomposition and intermediate formation of the respective imides and nitrides, respectively, proceed at quite low temperatures.<sup>24</sup> Figure 3 shows the high-temperature in situ X-ray diffractometry of  $M(NH_2)_2$  with  $M = Eu, Sr, Ba$ . For europium amide thermal decomposition leads to the formation of  $EuN$  at temperatures as low as 205 °C, indicated by the complete disappearance of the  $Eu(NH_2)_2$  reflections and appearance of europium nitride reflections at 14.1 and 16.3  $2\theta$  (JCPDS 15-887). With this method, no intermediate  $EuNH$  was observed, underlining a spontaneous and complete decomposition to  $EuN$  as suggested by Imamura et al.<sup>24</sup> In agreement with DTA/TG measurements no further degradation (up to 700 °C) was observed. The decomposition of  $Sr(NH_2)_2$  and  $Ba(NH_2)_2$  was also investigated, indicating thermal degradation and formation of the respective metal imides, without any byproducts, at 550 °C and 300 °C, respectively (Figure 3). In comparison with the in situ X-ray diffractometry, the DTA/TG measurements (Figure 4) indicated the formation of  $Sr(NH)$  at 100 °C lower temperatures. This is probably due to the fact that the imides

(22) Senker, J.; Jacobs, H.; Müller, M.; Press, W.; Müller, P.; Mayer, H. M.; Ibberson, R. M. *J. Phys. Chem. B* **1998**, *102*, 931.

(23) Linde, G.; Juza, R. *Z. Anorg. Allg. Chem.* **1974**, *409*, 199.

(24) Imamura, H.; Sakata, Y.; Tsuruwaka, Y.; Mise, S. *J. Alloys Compd.* **2006**, *408–412*, 1113.



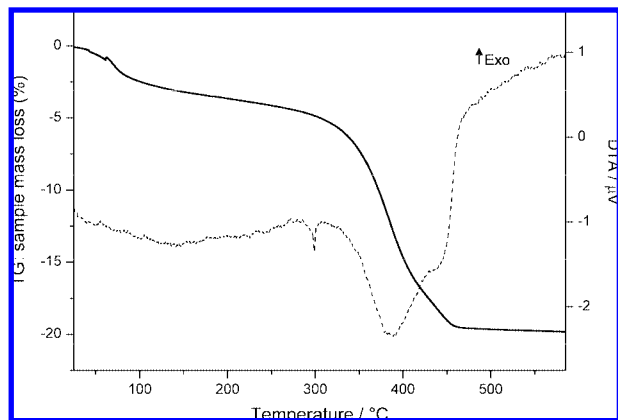


Figure 4. DTA (dotted line) and TG (solid line) measurement of  $\text{Sr}(\text{NH}_2)_2$ .

initially are formed as amorphous or nanocrystalline intermediates which undergo subsequent crystallization before they appear in the XRD pattern at somehow higher temperatures. The metal amides  $\text{M}(\text{NH}_2)_2$  ( $\text{M} = \text{Eu}, \text{Sr}, \text{Ba}$ ) are air sensitive and undergo rapid hydrolysis and formation of the respective hydroxides releasing ammonia.

The thermal behavior of these metal amides predestine them to be excellent starting materials for the synthesis of nitridosilicates (e.g., the 2-5-8 phosphor materials) due to their low decomposition temperature, their feature to release only hydrogen and nitrogen during the degradation process without any further byproducts, and the structural preorganization of the respective metal nitride. As already outlined, the metal amides can be synthesized at quite low temperatures (150 °C) and are thus much more reactive as compared to the metal nitrides which are usually obtained above 550 °C (Ba nitride) or 800 °C (Sr nitride and Eu nitride). Additionally, the nitrogen content in relation to the metal varies in the nitrides ( $\text{BaN}_x$  ( $x = 0.6$ );  $\text{SrN}_x$  ( $x = 0.6$ );  $\text{EuN}_x$  ( $x = 0.94$ )) depending on the synthesis conditions under flowing nitrogen.<sup>10</sup> The metal amides on the other hand are line compounds without phase width. Consequently, the latter ones can be easily employed as starting materials for subsequent synthesis of 2-5-8 phosphors in carefully measured amounts.

The classical synthesis of the nitridosilicates  $\text{M}_2\text{Si}_5\text{N}_8$  ( $\text{M} = \text{Eu}, \text{Sr}, \text{Ba}$ ) employs the reaction of the respective metals with silicon diimide  $\text{Si}(\text{NH}_2)_2$  under nitrogen atmosphere.<sup>14,15</sup> Thereby, the metal nitrides are initially formed as intermediates, subsequently reacting with  $\text{Si}(\text{NH}_2)_2$  to form the 2-5-8 phases. When the metal amides are used as starting materials, nitridation is no longer required. Accordingly, the temperature for the reaction with silicon diimide can be lowered significantly, possibly down to values of 900–1000 °C, where the decomposition of  $\text{Si}(\text{NH}_2)_2$  and subsequent formation of amorphous silicon nitride is observed.<sup>16</sup>

To investigate the reaction behavior of the metal amides with silicon diimide a number of various temperature programs were carried out using a radio-frequency furnace (Scheme 1). Special attention was directed to the reaction temperature **A**, the annealing time **B**, and the cooling rate **C**. Optimization of these parameters with the objective of performing low temperature synthesis for phase pure  $\text{M}_2\text{Si}_5\text{N}_8$

Scheme 1. Temperature Program Used for the Syntheses of  $\text{M}_2\text{Si}_5\text{N}_8$  ( $\text{M} = \text{Eu}, \text{Sr}, \text{Ba}$ )

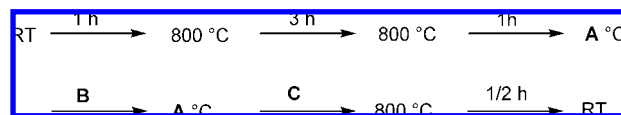


Table 1. Optimized Synthesis Conditions for Spherical Crystallites

compound	temperature	annealing time	cooling time
$\text{Eu}_2\text{Si}_5\text{N}_8$	1150 °C	6 h	12 h
$\text{Sr}_2\text{Si}_5\text{N}_8$	1200 °C	2–6 h	24 h
$\text{Ba}_2\text{Si}_5\text{N}_8$	1300–1400 °C	24 h	12 h

( $\text{M} = \text{Eu}, \text{Sr}, \text{Ba}$ ) and obtaining spherical crystallites was carried out. The optimized reaction parameters are summarized in Table 1. The experiments confirmed the high reactivity of  $\text{Eu}(\text{NH}_2)_2$  with silicon diimide; thus, a short annealing time of 6 h at 1150 °C is sufficient for complete reaction forming phase pure  $\text{Eu}_2\text{Si}_5\text{N}_8$  without the requirement of intermediate grinding. The obtained powder was investigated by powder XRD and the composition confirmed by EDX analysis. Further lowering of the synthesis temperature resulted in incomplete reactions, forming unknown byproducts and a high amorphous background in the XRD pattern, presumably caused by non-reacted silicon diimide. Compared to common synthesis routes employing Eu metal or nitride, which usually require temperatures around 1500–1600 °C,<sup>15</sup> this precursor approach can lower the maximum reaction temperatures by more than 300 °C. An analogous approach was applied to the synthesis of  $\text{Sr}_2\text{Si}_5\text{N}_8$  and  $\text{Ba}_2\text{Si}_5\text{N}_8$ , starting from the respective metal amides. The lowest maximum reaction temperature for formation of phase pure  $\text{Sr}_2\text{Si}_5\text{N}_8$  turned out to be 1200 °C with an annealing time of 2–6 h while the synthesis of single phase  $\text{Ba}_2\text{Si}_5\text{N}_8$  required slightly higher temperatures (1300–1400 °C) and a longer reaction time (>24 h).

To the best of our knowledge this precursor route starting from the metal amides yields phase pure and crystalline nitridosilicates  $\text{M}_2\text{Si}_5\text{N}_8$  ( $\text{M} = \text{Eu}, \text{Sr}, \text{Ba}$ ) at the lowest temperatures achieved so far. The recently reported synthesis of  $\text{M}_2\text{Si}_5\text{N}_8$  ( $\text{M} = \text{Sr}, \text{Ba}$ ) using metal nitrides required temperatures around 1300–1400 °C and additionally required two firing steps with intermediate grinding.<sup>25</sup>

**Morphology.** The influence of these low reaction temperatures on the crystal shape and size (morphology) of the nitridosilicate phases  $\text{M}_2\text{Si}_5\text{N}_8$  ( $\text{M} = \text{Eu}, \text{Sr}, \text{Ba}$ ) has been studied systematically. For this purpose, the products obtained by different reaction conditions have been investigated and compared by SEM measurements. Figure 5 shows SEM images of  $\text{Eu}_2\text{Si}_5\text{N}_8$  and  $\text{Sr}_2\text{Si}_5\text{N}_8$  recorded after different annealing temperatures, reaction times, and cooling rates. The experiments exhibit that high temperatures of ~1200 °C (Figure 5 a; Eu-2-5-8) implicate the formation of well formed and much bigger crystals with sharp edges and vertices. At lower temperatures of 1150 °C, a more uniform product with smaller crystallites and smoother edges was

(25) Li, Y. Q.; van Steen, J. E. J.; van Kreveld, J. W. H.; Botty, G.; Delsing, A. C. A.; DiSalvo, F. J.; deWith, G.; Hintzen, H. T. *J. Alloys Compd.* **2006**, *417*, 273.

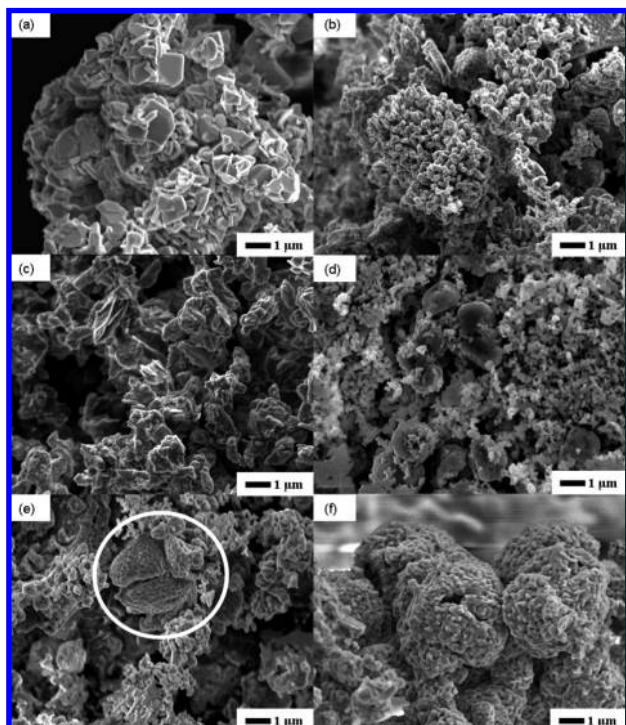


**Figure 5.** SEM images of  $\text{Eu}_2\text{Si}_5\text{N}_8$  with synthesis temperatures of 1200 °C (a) and 1150 °C (b);  $\text{Eu}_2\text{Si}_5\text{N}_8$  after annealing times of 2 h (c) and 6 h (d);  $\text{Eu}_2\text{Si}_5\text{N}_8$  with cooling rates of 6 h (e) and 24 h (f);  $\text{Sr}_2\text{Si}_5\text{N}_8$  with cooling rates of 24 h (f).

obtained for Eu-2-5-8 (Figure 5b), underlining a rather strong dependence of the maximum temperature on the morphology. Similar effect on the morphology could be observed for Sr-2-5-8 by application of a slightly higher reaction temperature (1200 °C, not depicted). Short annealing times of 2 h (Figure 5c, Eu-2-5-8) at 1150 °C resulted in the formation of coarser particles with sharp edges compared to firing of 6 h (Figure 5d) where a clear tendency to rounded particles can be observed. By extending the cooling rate to 6 h an increasing agglomeration rate can be detected as marked in Figure 5e (Eu-2-5-8). Nevertheless, the agglomerated particles with a size around 100 nm can still be recognized. Particularly, Figure 5f (Sr-2-5-8; cooling rate 24 h) shows the formation of large spherical structures formed out of small globular particles which are still visible in the SEM image. These investigations corroborate the possibility to form tailor-made crystallites by adjusting the temperature, annealing time, and cooling rate and revealed similar reaction behavior for Eu-2-5-8 and Sr-2-5-8.

The temperature program in Scheme 1 includes a pre-annealing step at 800 °C for 3 h. This step is not required for the formation of the nitridosilicates but appears to be of significance for the crystal morphology of the products. Figure 6a shows the SEM image of Sr-2-5-8 without annealing at 800 °C but directly heating to the synthesis temperature of 1200 °C. An obvious tendency to the formation of crystallites with clearly defined and sharp edges can be detected. This investigation emphasizes the importance of pre-annealing to achieve complete decomposition of the amide precursors, forming the metal nitrides. By applying this precursor route to the synthesis of  $\text{Ba}_2\text{Si}_5\text{N}_8$  a slightly different reactivity of the barium compound can be

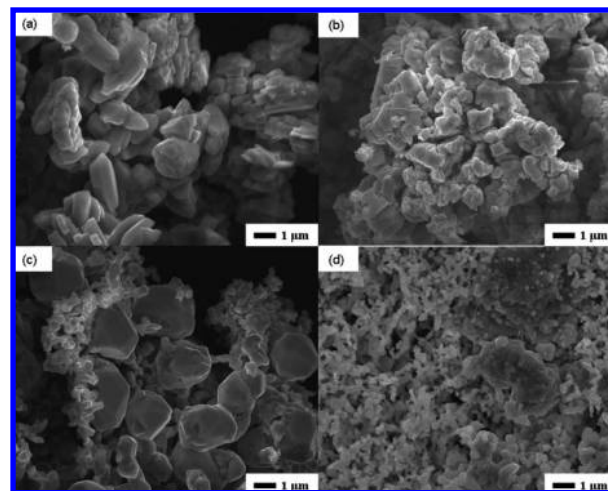


**Figure 6.** SEM images  $\text{Sr}_2\text{Si}_5\text{N}_8$  without pre-annealing at 800 °C;  $\text{Ba}_2\text{Si}_5\text{N}_8$  with synthesis temperatures of 1400 °C and annealing times of 6 h (b) and 24 h (c);  $\text{Ba}_2\text{Si}_5\text{N}_8$  with annealing times of 24 h and cooling rates of 12 h (d).

observed. Higher temperatures of about 1400 °C are required to achieve reasonable results. The obtained particles at annealing times of 6 h (Figure 6b) are forming agglomerated structures with crystallites exhibiting sharp edges. After extending these annealing times to 24 h the formation of the desired small particles with smoother edges can be detected (Figure 6c). However, large globular crystallites are visible in the SEM image. By combining long annealing times of 24 h with long cooling rates of 12 h a clear tendency to smaller and spherical particles (size of 100–200 nm) can be detected (Figure 6d). Longer annealing times result in more spherical and “softer” structures, but yielding particles of bigger size. This can be counteracted by extended cooling rates leading to small, spherical crystallites. Further investigations about this fact are currently ongoing.

**Europium Amide as Dopant.** As mentioned above, the 2-5-8 phases found application as  $\text{Eu}^{2+}$  doped luminescent materials.<sup>6,8,11–13</sup> To synthesize homogeneous phases  $\text{M}_2\text{Si}_5\text{N}_8$ :  $\text{Eu}^{2+}$ , mixtures of  $\text{Sr}(\text{NH}_2)_2$  or  $\text{Ba}(\text{NH}_2)_2$  together with  $\text{Eu}(\text{NH}_2)_2$  have been reacted with silicon diimide, and the influence of  $\text{Eu}(\text{NH}_2)_2$  as a dopant on the crystal morphology was investigated. For comparison different doping agents were applied, and the effect on the morphology of the particles was examined.<sup>26</sup> Each sample in the system  $\text{Ba}_2\text{Si}_5\text{N}_8$ :  $\text{Eu}^{2+}$  was doped with 1% europium (Figure 7). When doping with europium metal broad platelets and rods can be observed in the SEM image (Figure 7a and inset). In contrast, doping with europium oxide or europium halides leads to thin platelets, bar-like rods, and needles, respectively (Figure 7b,c). Figure 7d shows  $\text{Ba}_2\text{Si}_5\text{N}_8$  doped with 1%  $\text{Eu}(\text{NH}_2)_2$ . A clear tendency to spherically shaped crystallites can be observed, and no rods with sharp edges were found. Furthermore, a significant decrease in particle size to approximately 10% of the original length is observable. These investigations underline the influence of the doping agent on the crystallinity of the 2-5-8 phosphor materials in conjunction with lower synthesis temperatures. Additionally, the finely crystalline  $\text{Eu}(\text{NH}_2)_2$  can be mixed easily with the

(26) Stadler, F. Doctoral thesis, University of Munich (LMU), 2006.



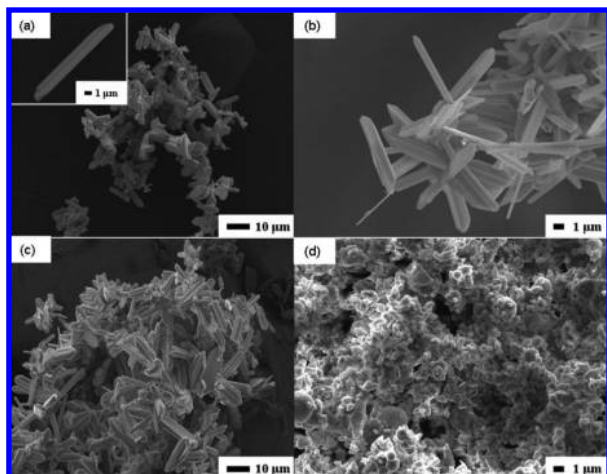


**Figure 7.** SEM images of  $\text{Ba}_2\text{Si}_5\text{N}_8:\text{Eu}^{2+}$  doped with europium metal (a),  $\text{EuF}_3$  (b),  $\text{Eu}_2\text{O}_3$  (c), and  $\text{Eu}(\text{NH}_2)_2$  (d).

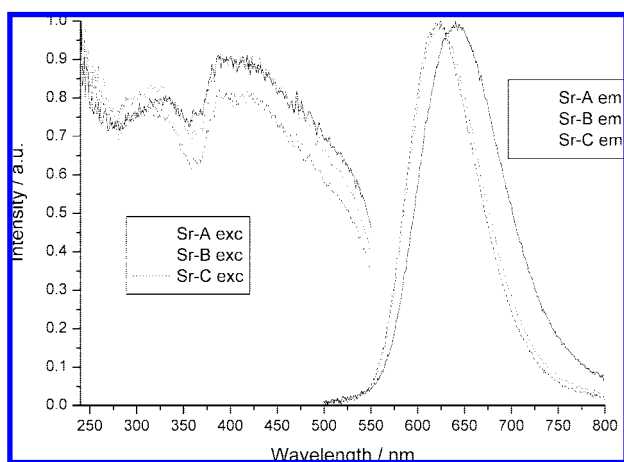


**Figure 8.** Photoluminescence spectra of  $\text{Sr}_2\text{Si}_5\text{N}_8:\text{Eu}^{2+}$  ( $\lambda_{\text{exc}} = 450 \text{ nm}$ ).

starting materials, leading to homogeneous doping. Furthermore, no halides are present to interfere with the starting materials, and therefore the problem with impurities is reduced.

**Luminescence.** The luminescence properties of  $\text{Eu}^{2+}$  doped  $\text{Sr}_2\text{Si}_5\text{N}_8$  and  $\text{Ba}_2\text{Si}_5\text{N}_8$  were determined with special attention to the influence of the synthesis temperature and the annealing time. Figure 8 illustrates photoluminescence spectra of three  $\text{Sr}_2\text{Si}_5\text{N}_8$  phosphor powders doped with 2%  $\text{Eu}^{2+}$ . The samples Sr-A and Sr-B differ in the synthesis temperature; Sr-A and Sr-C vary in their annealing times (Table 2). The excitation spectra cover the well-known broad range from the ultraviolet to the blue region. In the emission spectra a variation in the emission maximum can be observed which can be attributed to the varied synthesis conditions. The samples Sr-B and Sr-C show very similar broadband emission with maxima peaking at 625 nm and 624 nm, respectively. The emission wavelength of the well known  $5d^14f^6-4f^7$  transition of  $\text{Eu}^{2+}$  is typical for  $\text{Sr}_2\text{Si}_5\text{N}_8:\text{Eu}^{2+}$  and has already been described elsewhere.<sup>6</sup> The full width at half maximum (FWHM) of the emission band is also quite similar (Sr-B: 88 nm, Sr-C: 91 nm). However, sample Sr-A exhibits a red shift of the emission peak to 641 nm as well as an increase of the FWHM to 105 nm. To some extent this red shift could be generated by slightly higher europium

content within the sample. The optical parameters of the  $\text{Sr}_2\text{Si}_5\text{N}_8:\text{Eu}^{2+}$  samples obtained by the low-temperature precursor route have been measured at RT with excitation at 450 nm and compared to a reference sample of  $\text{Sr}_2\text{Si}_5\text{N}_8:\text{Eu}^{2+}$ , synthesized by standard methods (Table 2). Samples Sr-B and Sr-C exhibit CIE color coordinates quite similar to the reference sample accompanied by very good values for lumen equivalent and quantum efficiency. The good optical properties of sample Sr-B can be related to the highest synthesis temperature used in these investigations. Compound Sr-A, synthesized at the lowest temperature and with short annealing time, exhibits different CIE color coordinates, accompanied by lower quantum efficiency compared to the other samples. This decrease in efficiency is probably due to the presence of more defects in the host lattice. However, by extending the annealing time (e.g., Sr-C) good quantum efficiency and luminous equivalents can be achieved. Therefore, by combining longer annealing times with low temperatures both spherically shaped phosphor particles and competitive luminescence properties can be accomplished. This is probably due to the fact that impurities which can act as electron traps in the solid can be annealed by this way.

Analogously, the optical properties of three samples of  $\text{Ba}_2\text{Si}_5\text{N}_8:\text{Eu}^{2+}$  were measured. An experimental approach similar to that of the strontium compound was chosen (Table 3). Thus, samples that differ in synthesis temperature (Ba-A and Ba-B) and in annealing times (Ba-A, Ba-B, and Ba-C) were examined (Figure 9). The excitation curves cover the well known broad range from ultraviolet to blue-light region. When excited at 450 nm the emission peak center occurs at 581 nm and 585 nm for Ba-A and Ba-C, respectively. Ba-B shows a slight red shift to an emission maximum at 589 nm. The emission of Ba-A exhibits the smallest FWHM with 71 nm and a very steep decrease of the curve in the red region. Ba-B and Ba-C show a larger FWHM of 92 nm and 79 nm, respectively, and a noticeable tailing into the red region. The sample Ba-A shows very similar values compared to the reference whereas the compounds Ba-B and Ba-C exhibit different color coordinates and much lower lumen equivalents (cf. Table 3). The largest difference from the reference can be observed in Ba-B with quantum efficiency of only 35.6%. Good luminescence parameters can therefore be achieved by higher synthesis temperature and also by combining longer annealing times with lower synthesis temperatures. For  $\text{Ba}_2\text{Si}_5\text{N}_8:\text{Eu}^{2+}$  the optical properties of the sample Ba-A even surpass the results of Ba-C.

These investigations demonstrate that the most important parameter for good luminescence properties and spherical crystallites is the annealing time. Accordingly, the worse luminescence properties of products obtained at low temperature can be overcome by increased annealing times. Even without intermediate grinding and post-annealing these spherical shaped phosphor crystallites can compete with the phosphors obtained by the common synthesis route.

## Conclusion

In this contribution we report on a new low-temperature approach to the nitridosilicate phosphors  $\text{M}_2\text{Si}_5\text{N}_8:\text{Eu}^{2+}$  (M

**Table 2. Different Synthesis Conditions and Optical Properties of Sr<sub>2</sub>Si<sub>5</sub>N<sub>8</sub>:Eu<sup>2+</sup>**

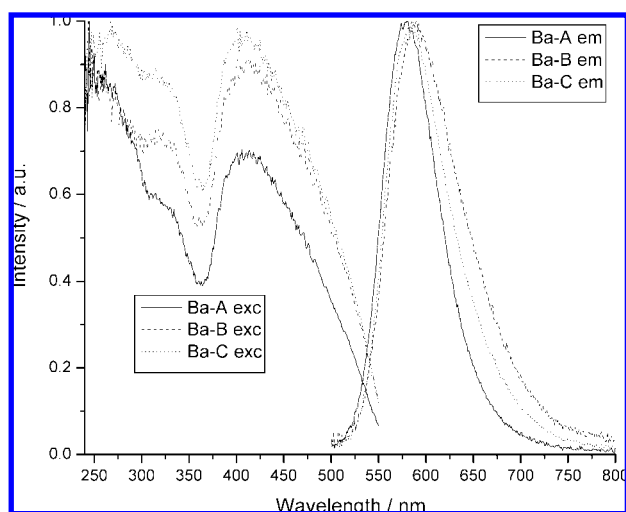
phase	temperature	annealing time	cooling time	$\lambda_{\text{emission}}$ [nm]	CIE color coordinates		lumen equivalent [lm/W]	rel. quantum efficiency [%]
					x	y		
Sr-A	1200 °C	6 h	12 h	641	0.645	0.353	147.2	68
Sr-B	1250 °C	6 h	12 h	625	0.629	0.370	225.3	75
Sr-C	1200 °C	12 h	12 h	624	0.631	0.368	212.5	72
reference sample	1550 °C	6 h	12 h	625	0.634	0.365	215.0	100

**Table 3. Different Synthesis Conditions and Optical Properties of Ba<sub>2</sub>Si<sub>5</sub>N<sub>8</sub>:Eu<sup>2+</sup>**

phase	temperature	annealing time	cooling time	$\lambda_{\text{emission}}$ [nm]	CIE color coordinates		lumen equivalent [lm/W]	rel. quantum efficiency [%]
					x	y		
Ba-A	1300 °C	24 h	12 h	581	0.516	0.481	457.8	79
Ba-B	1300 °C	6 h	12 h	589	0.553	0.445	348.4	42
Ba-C	1400 °C	12 h	12 h	585	0.539	0.459	349.2	77
reference sample <sup>26</sup>	1550 °C	6 h	12 h	580	0.515	0.482	472.0	100

= Sr, Ba) for white light emitting diodes. The experimental procedure includes the use of reactive metal amide precursors synthesized by dissolving and reacting the metals in supercritical ammonia. The thermal behavior of these precursors was studied by high temperature in situ X-ray diffractometry, DTA/TG measurements, and IR-measurements. The amides have proven to be excellent starting materials for the synthesis of nitridosilicates due to their high reactivity and thermal decomposition feasibility, leaving solely metal nitrides and imides already at low temperatures. This enables us to decrease the synthesis temperature of these nitridosilicates significantly up to 300 °C compared to common synthesis temperatures. Furthermore, the usage of these amide precursors in combination with appropriate temperature programs gives access to tailor made crystal morphology. Additionally, the use of Eu(NH<sub>2</sub>)<sub>2</sub> as dopant was investigated. Doping with this compound led to spherical particles with smooth edges compared to common doping agents. With the formation of spherically shaped crystallites it is possible to improve light extraction from the crystallites.

Due to the rather high refraction index of the 2-5-8 phases (between 2 and 3)<sup>27</sup> highly anisotropical crystal morphologies (high aspect ratio) are leading to total reflection and thus light guiding within the 2-5-8 phosphor material. Therefore an increasing re-absorption followed by an energy loss occurs for non-spherical crystallites. Additionally, we have shown that lower reaction temperatures do not have to result in worse optical properties if the annealing time is adjusted. Thereby, very good luminescence properties compared to commonly synthesized phosphor powders can be achieved. The highly reactive material obtained by our sc-NH<sub>3</sub> approach is specifically useful for further processing (e.g., thermally aftertreatment) to regain the typical optimized properties of the 2-5-8 phosphors (e.g., quantum efficiencies up to 100%, low thermal quenching). This is very promising for further industrial and scientific applications and will allow for the design of more efficient warm white LEDs by simultaneously decreasing the reaction temperatures. The applicability of the sc-NH<sub>3</sub> approach in industrial approaches cannot be answered as yet. However, the industrial value creation of LED phosphors is rather high. Presumably, the use of reactive amide precursors can be successfully applied to the synthesis of other nitridosilicates.

**Figure 9.** Photoluminescence spectra of Ba<sub>2</sub>Si<sub>5</sub>N<sub>8</sub>:Eu<sup>2+</sup> ( $\lambda_{\text{exc}} = 450$  nm).

**Acknowledgment.** We thank A. Sattler for conducting the DTA/TG measurements, as well as T. Miller for collecting the high temperature in situ X-ray diffraction data. Special thanks are directed to Dr. P. Schmidt (Philips Technology GmbH Research laboratories Aachen) for performing luminescence measurements. The authors gratefully acknowledge financial support by the Fonds der Chemischen Industrie (FCI).

**Supporting Information Available:** IR-spectra of M(NH<sub>2</sub>)<sub>2</sub> (M = Ba, Eu) and XRD pattern (Mo K $\alpha_1$ ) of M<sub>2</sub>Si<sub>5</sub>N<sub>8</sub> (M = Eu, Sr, Ba) (PDF). This material is available free of charge via the Internet at <http://pubs.acs.org>.

CM8024796

(27) Lutz, H.; Joosten, S.; Hoffmann, J.; Lehmeier, P.; Seilmeier, A.; Höpfe, H. A.; Schnick, W. *J. Phys. Chem. Solids* **2004**, *65*, 1285.